MOLECULAR AND CELLULAR BIOLOGY, Jan. 1993, p. 506–520
0270-7306/93/130506-15$02.00/0

Vol. 13, No. 1

GCD11, a Negative Regulator of *GCN4* Expression, Encodes the γ Subunit of eIF-2 in *Saccharomyces cerevisiae*

ERNEST M. HANNIG,[1]* A. MARK CIGAN,[2] BARBARA A. FREEMAN,[1] AND TERRI GOSS KINZY[3]

Molecular and Cell Biology Program, The University of Texas at Dallas, P.O. Box 830688, Richardson, Texas 75083-0688[1]; Section on Molecular Genetics of Lower Eukaryotes, Laboratory of Molecular Genetics, National Institute of Child Health and Human Development, Bethesda, Maryland 20892[2]; and Department of Biochemistry, School of Medicine, Case Western Reserve University, Cleveland, Ohio 44106[3]

Received 22 July 1992/Returned for modification 8 September 1992/Accepted 12 October 1992

The eukaryotic translation initiation factor eIF-2 plays a critical role in regulating the expression of the yeast transcriptional activator *GCN4*. Mutations in genes encoding the α and β subunits of eIF-2 alter translational efficiency at the *GCN4* AUG codon and constitutively elevate *GCN4* translation. Mutations in the yeast *GCD11* gene have been shown to confer a similar phenotype. The nucleotide sequence of the cloned *GCD11* gene predicts a 527-amino-acid polypeptide that is similar to the prokaryotic translation elongation factor EF-Tu. Relative to EF-Tu, the deduced GCD11 amino acid sequence contains a 90-amino-acid N-terminal extension and an internal cysteine-rich sequence that contains a potential metal-binding finger motif. We have identified the *GCD11* gene product as the γ subunit of eIF-2 by the following criteria: (i) sequence identities with mammalian eIF-2γ peptides; (ii) increased eIF-2 activity in extracts prepared from cells cooverexpressing GCD11, eIF-2α, and eIF-2β; and (iii) cross-reactivity of antibodies directed against the GCD11 protein with the 58-kDa polypeptide present in purified yeast eIF-2. The predicted GCD11 polypeptide contains all of the consensus elements known to be required for guanine nucleotide binding, suggesting that, in *Saccharomyces cerevisiae*, the γ subunit of eIF-2 is responsible for GDP-GTP binding.

General amino acid control in the yeast *Saccharomyces cerevisiae* is a regulatory pathway that acts to coordinately derepress the transcription of at least 30 unlinked amino acid biosynthetic genes, involved in 10 pathways, in cells starved for a single amino acid. This cross-pathway response is mediated by the transcriptional activator GCN4, whose target sequences are located upstream from the coregulated biosynthetic genes. The level of GCN4 protein increases in response to amino acid starvation due to increased translation of the *GCN4* coding sequences. Translational regulation of *GCN4* is mediated in *cis* by four short upstream open reading frames (uORFs), present in the leader sequences of the *GCN4* mRNA, that inhibit translation of downstream *GCN4* coding sequences. Multiple positive and negative *trans*-acting regulators of *GCN4* expression have been identified by genetic analyses. Negative effectors (*GCD* gene products) promote the inhibitory effects of the uORFs on translation of *GCN4* coding sequences. Positive effectors encoded by *GCN1*, *GCN2*, and *GCN3* antagonize the function of *GCD* genes in starved cells and promote increased translation of *GCN4* coding sequences under these conditions. Results of genetic and biochemical analyses indicate that translational regulation of GCN4 synthesis by GCN and GCD *trans*-acting factors occurs at the initiation step of protein synthesis (for a review, see reference 32).

Initiation of protein synthesis in eukaryotic organisms is a complex process involving the small (40S) ribosomal subunit and multiple protein factors (eukaryotic initiation factors, eIF) that cycle on and off the small subunit with each round of initiation (for a review, see references 30, 45, and 48). Briefly, a 40S subunit, bound with eIF-1A, eIF-3, and a ternary complex of eIF-2, GTP, and the methionine initiator tRNA, recognizes an mRNA (which is bound by an additional set of initiation factors) and attaches at or near its 5′ capped end. The factor-bound 40S subunit then scans the mRNA linearly in a 5′-to-3′ direction until it encounters an AUG translation initiation codon in a favorable context (41). Upon reaching the start codon, GTP is hydrolyzed, Met-tRNA$_i$ is donated to the ribosomal half-P site, and eIF-1A, eIF-3, and eIF-2–GDP are released from the 40S subunit in a reaction promoted by eIF-5. The eIF-2–GDP complex formed as a result of GTP hydrolysis must be converted to the GTP-bound form to allow eIF-2 to bind Met-tRNA$_i$ and participate in a subsequent round of initiation. The reaction in which GTP is exchanged for the GDP bound to eIF-2 is catalyzed by the guanine nucleotide exchange factor eIF-2B.

In both amino acid-starved and unstarved cells, it appears that ribosomes initiate protein synthesis at the AUG codon of the 5′-proximal uORF (uORF1) on *GCN4* mRNA, terminate three codons downstream at an in-frame termination codon, and dissociate from the mRNA. There is evidence, however, that about one-half of the 40S subunits that terminate at uORF1 remain associated with the *GCN4* mRNA and resume scanning (1). Abastado et al. (1) have suggested that in rapidly growing (unstarved) cells, these 40S subunits quickly reacquire protein factors and reinitiate translation at the AUG codon of one of the remaining downstream uORFs. Initiation and subsequent termination at these uORFs lead to essentially complete dissociation of 80S ribosomes from the *GCN4* mRNA (1, 49). Amino acid starvation results in reduced reinitiation at uORFs 2, 3, and 4 and increased reinitiation at the *GCN4* AUG codon, perhaps because of a decrease in the activity of one or more initiation factors (1).

Genetic and molecular analyses have identified the initiation factor eIF-2 as a key regulator of *GCN4* expression. In *S. cerevisiae*, as well as in mammals, eIF-2 is composed of three nonidentical subunits termed α (36 kDa), β (38 kDa),

* Corresponding author.

TABLE 1. *S. cerevisiae* strains

Strain	Genotype	Source or reference
EY250	*MAT***a** *gcd11-508 gcn2-101 gcn3-101 ura3-52*	This study
EY252	*MAT***a** *gcd11-508 gcn3-101 leu2-3 leu2-112 ura3-52* (*HIS4*::*lacZ URA3*$^+$)	This study
EY307	*MAT***a** *gcn3-101 leu2-3 leu2-112 ura3-52*	This study
EY424[a]	*MAT***a** *gcn3-101 leu2-3 leu2-112 ura3-52* (Ep274 integrated at *GCD11*, Leu$^+$)	This study
EY482[b]	*MAT*α *leu2-3 leu2-112 ino1 pep4*::*URA3 ura3-52* (*HIS4*::*lacZ ura3-52*)	P. Miller and A. Hinnebusch
EY563	*MAT***a** *gcd11-508 gcn3-101 leu2-3 leu2-112 ura3-52* (*HIS4*::*lacZ ura3-52*) *GAL2*	This study
F35	*MAT***a** *ino1 can1 ura3-52* (*HIS4*::*lacZ URA3*$^+$)	46
H4	*MAT***a** *leu2-3 leu2-112 ura3-52*	24
H117[c]	*MAT***a** *gcn2-101 gcn3-101 ino1 his1-29 ura3-52* (*HIS4*::*lacZ URA3*$^+$)	28
H227	*MAT***a** *leu2-3 leu2-112 ura3-52 GAL2*	A. Hinnebusch
H272[c]	*MAT***a** *gcd11-508 gcn2-101 gcn3-101 ino1 his1-29 ura3-52* (*HIS4*::*lacZ URA3*$^+$)	28
H1402	*MAT*α *leu2-3 leu2-112 ino1 ura3-52* (*HIS4*::*lacZ ura3-52*)	26
S288C	*MAT*α	

[a] Isogenic with EY307.
[b] Isogenic with H1402.
[c] Isogenic strains.

and γ (55 kDa) (for a review, see reference 48). Mutations in essential genes encoding the α (*SUI2*) and β (*SUI3*) subunits of eIF-2 in yeast constitutively derepress *GCN4* translation (a Gcd$^-$ phenotype), indicating that eIF-2 acts as a negative regulator of *GCN4* expression (69). *GCN2* encodes a protein kinase that phosphorylates eIF-2α on serine residue 51 (15). This phosphorylation event is required for derepression of *GCN4* translation in amino acid-starved cells (15, 68). In other eukaryotic systems, phosphorylation of eIF-2α on serine 51 has been shown to reduce eIF-2 function by increasing the stability of the eIF-2–GDP–eIF-2B complex and sequestering limiting amounts of eIF-2B (for a review, see references 30, 45, and 48). Dever et al. (15) have proposed that phosphorylation of eIF-2 by GCN2 has the same effect in *S. cerevisiae*, leading to reduced levels of ternary complex in amino acid-starved cells. As a result, many of the 40S subunits that have resumed scanning downstream from uORF1 in the *GCN4* mRNA leader fail to bind ternary complex and fail to reinitiate at uORFs 2 to 4. Most of these 40S subunits reacquire ternary complex while scanning the uORF4-*GCN4* interval and reinitiate at the *GCN4* start codon. Mutations in *SUI2* and *SUI3* that lead to reduced eIF-2 function would, therefore, mimic the inhibitory effect of phosphorylation of eIF-2 and constitutively derepress *GCN4* translation. Mutations in *GCD1* and *GCD2*, essential genes that appear to encode subunits of eIF-2B (10), would likewise derepress the translation of *GCN4* by impairing GDP-GTP exchange on eIF-2.

We report here the isolation and characterization of the yeast *GCD11* gene. Harashima and Hinnebusch originally isolated mutant alleles of *GCD11* as suppressors of the inability to derepress *GCN4* expression associated with mutations in the positive regulators *GCN2* and *GCN3* (28). *gcd11* strains exhibit constitutive *GCN4* expression and an unconditional slow-growth phenotype. Genetic interactions between *GCD11* and *GCN3*, which appears to encode a subunit of eIF-2B (10, 24), suggested a physical interaction between GCN3 and the *GCD11* gene product (27). Analysis of the cloned *GCD11* gene suggests that the *GCD11* gene product is a GTP-binding protein with marked similarity to bacterial and mitochondrial EF-Tu. Biochemical analyses indicate that the GCD11 protein is the γ subunit of eIF-2 in *S. cerevisiae*.

MATERIALS AND METHODS

Strains and genetic techniques. *Escherichia coli* DH5α was used for plasmid propagation, strain RR1 was used for production of *trpE* fusion proteins, and strain DH5α F′ was used for propagation of M13 derivatives. Double-stranded plasmid and phage DNAs were introduced into bacterial strains by the method of Hanahan (23). 5-Fluoroortic acid (5-FOA) was purchased from PCR Incorporated. Minimal medium plates (SD) with 30 mM 3-amino-1,2,4-triazole (AT; Sigma) contained L-leucine at 40 mM and the remaining 18 L-amino acids (histidine is omitted) at 0.1 mg/ml. AT inhibits the *HIS3* gene product and elicits a histidine starvation. Gcn$^-$ strains that cannot derepress the general control fail to grow on AT-containing medium lacking histidine.

Yeast strains used in these studies are listed in Table 1. Strain constructions and yeast genetic analyses were performed by using standard techniques and media (63). All strains were derived from S288C. The *gcd11-508* allele in strain EY250 was derived from H272. The *GAL2* allele in EY563 was derived from H227. The presence of unmarked *gcn2* and *gcn3* alleles was confirmed by testing hybrids formed with appropriate tester strains for sensitivity to AT.

Plasmids were introduced into yeast strains by the lithium acetate method (35). For initial isolation of the *GCD11* gene from a yeast genomic library (58), the transformation mixtures were plated on minimal medium and the plates were incubated at 37°C. These conditions exacerbated the difference in the growth rate between YCp50 (vector) and *GCN3* (Ep69) transformants of EY250. Gene replacements were performed by the one-step method of Rothstein (59) with 4 to 5 μg of linear DNA purified by preparative gel electrophoresis and 20 μg of sheared calf thymus DNA as carrier.

Plasmids. Yeast-*E. coli* shuttle vectors used in these experiments were YCp50, pRS315, pRS316, YEp24, YEp13, and YIp32. YCp50 contains the yeast *URA3* gene as a selectable marker and the yeast *ARS1* and *CEN4* sequences for autonomous low-copy-number propagation in yeasts (36). pRS315 and pRS316 contain the yeast *ARSH4* and *CEN6* sequences and either the yeast *URA3* (pRS316) or the yeast *LEU2* (pRS315) gene as a selectable marker (64). YEp24 and YEp13 contain the yeast *URA3* (YEp24) or *LEU2* (YEp13) gene and the 2μm replication origin and are maintained autonomously at high copy numbers in yeast cells (7). YIp32 contains the yeast *LEU2* gene as a selectable

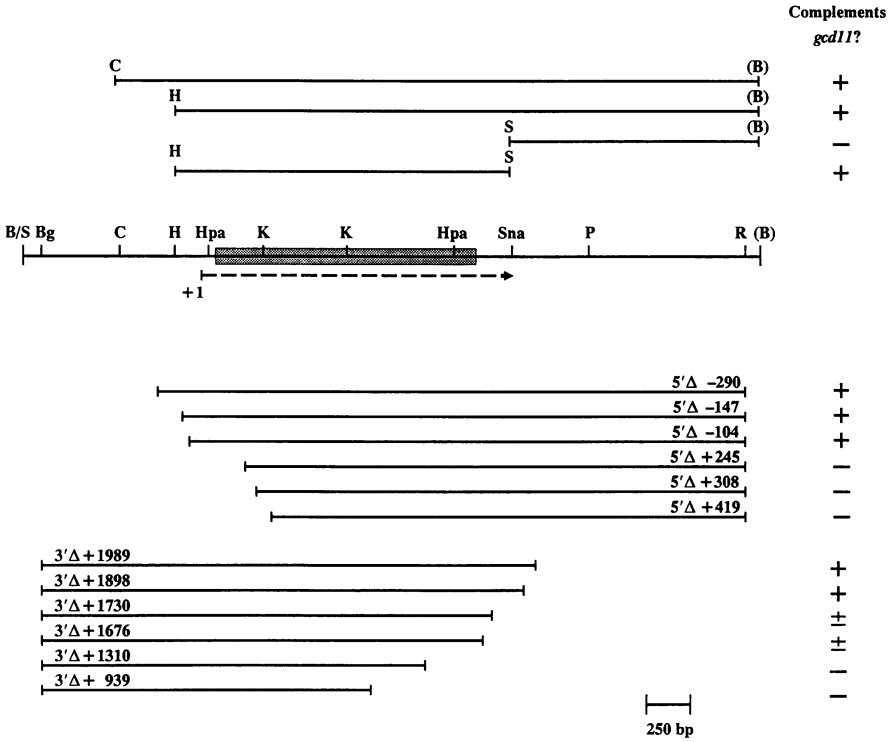

FIG. 1. Localization of *GCD11* complementation unit. Partial restriction map of the 4.5-kb genomic fragment cloned in Ep264 is shown, along with regions corresponding to the 1.58-kb *GCD11* ORF (shaded) and the 1.9-kb *GCD11* transcript (arrow). +1 indicates the farthest upstream start site determined for the *GCD11* transcript. Lines above the restriction map correspond to fragments tested separately as subclones in YCp50 for complementation in EY250. Deletion alleles used in complementation testing are shown below the partial restriction map; lines correspond to DNA present in each deletion subclone. Complementation refers to the ability to alleviate the growth defect and to unmask the *gcn* mutations in EY250. Symbols: +, strong complementation; +/−, weak complementation; −, no complementation. Restriction enzymes: (B), *Bam*HI; B/S, *Bam*HI-*Sau*3A junction; Bg, *Bgl*II; C, *Cla*I, H, *Hin*dIII; Hpa, *Hpa*I; K, *Kpn*I; P, *Pvu*II; R, *Eco*RI; Sna, *Sna*BI.

marker but lacks sequences required for autonomous replication in yeast cells (7). Plasmid Ep69 is a YCp50-based plasmid that contains the wild-type yeast *GCN3* gene (24). Plasmid TD14-6 (provided by T. Dever, National Institutes of Health) contains the *SUI2* (eIF-2α) and *SUI3* (eIF-2β) genes (provided by T. Donahue, Indiana University) on 2.4-kb *Bam*HI and 1.8-kb *Hin*dIII restriction fragments, respectively, inserted into YEp24.

Ep264, which contains the *GCD11* gene on a 4.5-kb genomic fragment (Fig. 1), was isolated from a yeast genomic library constructed in YCp50 (52). A unique *Bam*HI site in Ep264 is present at one of the insert-vector junctions. Ep274 contains a 4.3-kb *Bam*HI-*Bgl*II genomic fragment from Ep264 inserted at the *Bam*HI site of YIp32. The *Bgl*II site in the 4.0-kb *Eco*RI-*Bgl*II *GCD11* fragment from Ep264 was flush ended with Klenow enzyme and converted to an *Eco*RI site by the addition of a synthetic *Eco*RI linker. The resulting 4.0-kb *Eco*RI fragment was inserted in either orientation at the *Eco*RI site of YCp50 to create Ep359 and Ep360.

Ep272 contains the 4.3-kb *Bam*HI-*Bgl*II *GCD11* fragment derived from Ep264 inserted at the *Bam*HI site of YCp50. Ep272 was cleaved at a unique *Sna*BI site present in the *GCD11* sequences, and an unphosphorylated synthetic decanucleotide linker was inserted to create a new *Hin*dIII site in plasmid Ep286. A 2.1-kb *GCD11* *Hin*dIII fragment (extending from the genomic *Hin*dIII site to the genomic *Sna*BI site) was isolated from Ep286 and flush ended with Klenow enzyme, and a synthetic *Bam*HI linker octamer was added at each end. The resulting *Bam*HI fragment was inserted at the *Bam*HI site of YEp24 (to create Ep361) or YEp13 (to create plasmid BM35). Plasmid Ep358 was derived from Ep286 by digestion with *Eco*RI and removal of a 0.58-kb *Eco*RI fragment containing the *Hin*dIII site present in vector sequences. The *gcd11*::*URA3* (*Δ1-527*) allele in plasmid Ep363 was created by replacing the 2.1-kb *Hin*dIII *GCD11* fragment in plasmid Ep358 with a 1.1-kb *Hin*dIII fragment (24) containing the *URA3* gene. Ep415 contains the 2.1-kb *Hin*dIII *GCD11* fragment from Ep358 inserted at the unique *Hin*dIII site in pRS315.

pRS316 was linearized by digestion with *Kpn*I, the resulting 3′ single-stranded sequences were removed with Klenow enzyme, and the plasmid was religated to create Ep432. The *Bam*HI *GCD11* fragment from Ep361 was inserted at the *Bam*HI site of Ep432 to create Ep433. Plasmid Ep434 contains the *gcd11Δ106-273* allele and was constructed by cleavage of Ep433 with *Kpn*I, removal of the 0.5-kb *Kpn*I fragment containing *GCD11* sequences, and religation. Ep444 was created by cleaving Ep433 at one of the two *Kpn*I sites in the *GCD11* sequences. The 3′ single-stranded sequences were removed with Klenow enzyme, and the flush ends were religated. Removal of the 4 bp at positions +880 to +883 (Fig. 2) in Ep444 was verified by sequence analysis. Ep442, used in RNA mapping experiments, was constructed by insertion of the 1.6-kb *Bam*HI *GCD11* fragment from Ep434 at the *Bam*HI site of M13mp19 (71).

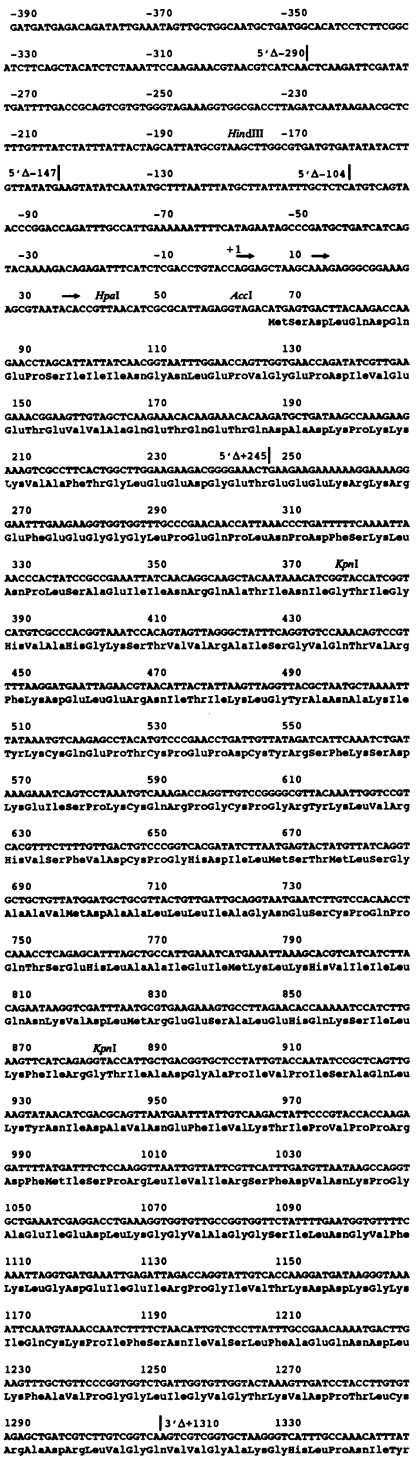

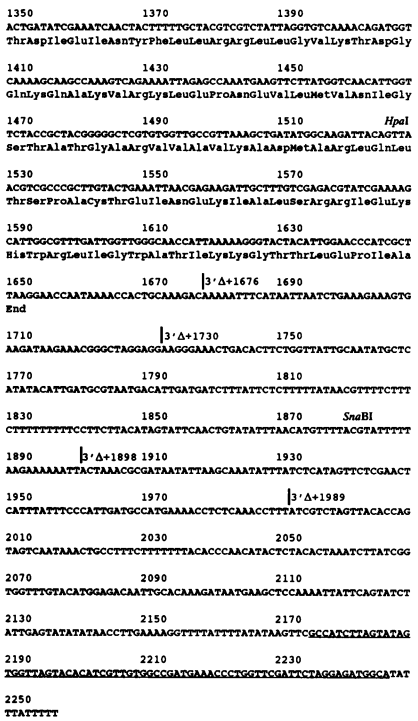

FIG. 2. DNA sequence analysis of *GCD11*. Nucleotide sequences from −378 to +2254 were determined on both strands. The predicted 527-amino-acid product of the single long ORF is listed beneath the nucleotide sequence, beginning at position +66 and extending to position +1646. Arrows indicate transcription start sites at +1, +12, and +35, as determined by S1 nuclease and primer extension analyses. Selected deletion junctions depicted in Fig. 1 are shown above the sequences. Sequences corresponding to a histidyl-tRNA are underlined (+2172 to +2243).

Construction of plasmids containing *trpE-GCD11* fusions was begun by insertion of the 2.1-kb *Hin*dIII *GCD11* fragment from Ep358 at the *Hin*dIII site of pUC19 to create Ep437. The orientation of the *GCD11* fragment in Ep437 was such that cleavage with *Xba*I (in polylinker sequences) and *Acc*I (which cleaves once in polylinker and once in insert sequences) removed a 0.26-kb fragment containing *GCD11* sequences −180 to +61 (Fig. 2). The single-stranded *Xba*I and *Acc*I 5′ ends were flush ended with Klenow enzyme, and the plasmid was religated to create Ep439. The sequences at the vector-insert junction, 5′-GGATCCTCTAGAGACATG-3′, were confirmed by sequence analysis. The ATG triplet (boldface) represents the putative *GCD11* translation initiation codon. A 1.8-kb *Bam*HI (underlined)-*Hin*dIII *GCD11* fragment was removed from Ep439 and ligated to *Bam*HI-*Hin*dIII-cleaved pATH3 (17) to create Ep448. In Ep448, the complete *GCD11* coding sequences are in frame with upstream *trpE* coding sequences and under the control of the *E. coli trpE* promoter. Ep448 was cleaved with *Kpn*I to remove the 0.5-kb *Kpn*I fragment containing *GCD11* coding sequences, and the plasmid was religated to create plasmid Ep449. Ep449 contains the *trpE-gcd11Δ106-273* allele.

Ep510 was constructed by converting the *Hin*dIII site in Ep439 to a *Bam*HI site, as above, and inserting the resulting 1.8-kb *Bam*HI-*GCD11* fragment at the *Bam*HI site of pBM150 (36). This construct places the transcription of the *GCD11* coding sequences under the control of the yeast *GAL1* promoter. Ep509 contains the same 1.8-kb *Bam*HI insert, in the opposite orientation.

Sequence analysis. Ep359 and Ep360 were cleaved with both *Bam*HI and *Sph*I, and unidirectional deletion alleles were constructed by the exonuclease III method (29). The deletion alleles were used as templates for nucleotide sequence analysis of *GCD11*. Double-stranded plasmid DNA was prepared by the alkaline lysis method and sequenced by using a Sequenase version 2.0 kit (U.S. Biochemicals), [α-^{32}P]dATP (specific activity, 3,000 Ci/mmol; ICN Bio-

medicals, Inc.), and the synthetic oligonucleotide primer 5′-GACGCTCTCCCTTATGCG-3′, corresponding to sequences between the unique *Sph*I and *Sal*I sites present in the YCp50 vector. The *GCD11* nucleotide sequence was determined on both strands by sequencing additional restriction fragment subclones and, in some cases, by utilizing additional synthetic oligonucleotide primers. Oligodeoxyribonucleotides were synthesized on an Applied Biosystems model 381A DNA synthesizer. Software by Microgenie (57) and the Genetics Computer Group (16) was used for computer analysis of DNA sequences.

DNA methods. Recombinant DNA manipulations were performed essentially as described elsewhere (61). Plasmids were recovered from total yeast DNA prepared as previously described (34) and isolated by introduction into competent *E. coli* DH5α. Total yeast DNA used for DNA blot hybridization (Southern blot) analysis was prepared essentially as described previously (66). DNA was digested with *Eco*RI prior to separation by agarose gel electrophoresis and transfer to nitrocellulose paper. Immobilized DNA was hybridized with the radiolabeled (19) 4.3-kb *Bam*HI-*Bgl*II-*GCD11* fragment isolated from Ep264 as previously described (65).

RNA methods. Yeast strains were cultured at 30°C in SD medium supplemented with 0.1 mM *myo*-inositol, 2 mM L-leucine, 0.5 mM L-isoleucine, 0.5 mM L-valine, and 0.2 mM uracil (when necessary), unless otherwise indicated. Cells were grown to saturation in supplemented SD medium and then diluted 1:50 into fresh medium and grown at 30°C and 300 rpm either for 8 h (repressed) or for 2 h followed by the addition of AT to 10 mM and growth for an additional 6 h (derepressed). The cells were harvested, and RNA was extracted as described previously (but without bentonite) (25). RNA blot hybridization (Northern) analysis was performed as previously described (31). The amount of total RNA was normalized to contain equivalent amounts of *PYK* mRNA. The *PYK* probe was a 6.7-kb *Hin*dIII fragment from plasmid pFR2 (provided by G. Fink). The *HIS4* probe was a 2.8-kb *Eco*RI fragment derived from pR5 (provided by P. Farabaugh). *GCD11* probes used were the 2.1-kb *Hin*dIII-*Sna*BI and the 1.5-kb *Hpa*I *GCD11* fragments, as described in Results.

Poly(A)$^+$ RNA was prepared from total RNA, extracted from strain S288C, by oligo(dT)-cellulose chromatography (25). For primer extension analyses, the synthetic oligonucleotide 5′-ATCTGGTTCACCAACTGGTTC-3′, which is complementary to nucleotides +137 to +117 (Fig. 2), was radiolabeled at its 5′ terminus with [γ-^{32}P]ATP (specific activity, 4,000 Ci/mmol; ICN Biomedicals, Inc.) and T4 polynucleotide kinase and purified by electrophoresis through an 8 M urea-20% polyacrylamide gel. Hybridization conditions and primer extension with avian myeloblastosis virus reverse transcriptase were as previously described (51). For S1 nuclease mapping experiments, the same 5′ radiolabeled oligonucleotide was hybridized with single-stranded phage DNA prepared from Ep442 and extended by using Sequenase version 2.0 T7 DNA polymerase. The double-stranded extension products were digested with *Hin*dIII, and a single-stranded, 5′-end-labeled DNA probe extending from +137 to −180 was purified by electrophoresis through 1.2% low-melting-temperature agarose at alkaline pH. S1 nuclease was titrated in preliminary experiments to determine optimal conditions (33). Primer extension and S1 nuclease products were compared with a sequencing ladder prepared by using the +137 to +117 5′-end-labeled oligonucleotide as a primer and single-stranded DNA derived from Ep442 as a template.

Production of GCD11-specific antisera. Antibodies against *trpE-GCD11* fusion proteins that were overproduced in *E. coli* RR1 harboring plasmid Ep448 (*trpE-GCD11*) or Ep449 (*trpE-gcd11Δ106-273*) were raised in female New Zealand White rabbits. Ep448 contains the complete *GCD11* coding sequences. The shorter fusion protein encoded by *trpE-gcd11Δ106-273* lacks 168 internal GCD11 amino acids that contain the majority of the consensus guanine nucleotide binding sequences (see Results). Fusion proteins were identified by comparison of the proteins present in total and insoluble fractions prepared from Ep448 and Ep449 transformants with those present in similar fractions prepared from strain RR1 and RR1 harboring the pATH3 vector.

On the basis of the deduced *GCD11* ORF, we predicted that fusion proteins of 95 and 76 kDa would be synthesized in *E. coli* from the *trpE-GCD11* and *trpE-gcd11Δ106-273* fusion constructs, respectively. The predicted masses are close to the relative masses of 98 and 78 kDa determined experimentally by sodium dodecyl sulfate (SDS)-polyacrylamide gel electrophoresis (data not shown). Fusion proteins were partially purified from an insoluble fraction by SDS-polyacrylamide gel electrophoresis as previously described (17). Gel slices containing approximately 250 μg (per rabbit per immunization) of fusion protein were emulsified with complete (primary immunization) or incomplete (booster) Freund's adjuvant (Sigma) and injected subcutaneously. Rabbits received booster immunizations 5 weeks after the primary immunization and subsequently at 4-week intervals. A single bleeding (50 ml) was performed 10 to 12 days after each boost. Serum was stored without preservatives at −70°C.

Analysis of steady-state levels of GCD11 protein. Cells were grown under repressing and derepressing conditions as described above. Extracts were prepared as follows. A 1.25-ml aliquot of culture was added to a chilled 1.5-ml tube containing 150 μl of 50% trichloroacetic acid. Tubes were mixed by inversion and kept at 0°C for 20 min. Cells were pelleted by centrifugation (15,000 × *g* for 10 min) at 4°C, rinsed twice with ice-cold acetone, and dried. Pellets were resuspended in 100 to 150 μl of 2× sample buffer (43) containing phenylmethylsulfonyl fluoride (0.1 mg/ml), aprotinin (1 μg/ml), leupeptin (0.5 μg/ml), and pepstatin (1 μg/ml). Acid-washed glass beads (0.55 mm) were added to the meniscus, cells were broken by vortexing at high speed for 1 min, and the cell lysates were immediately boiled for 4 min.

Aliquots of extract containing equivalent amounts of protein, as determined in preliminary experiments, were fractionated on SDS-polyacrylamide gels (43) and transferred to nitrocellulose paper. Blots were blocked, probed, and developed using either a conjugated secondary antibody and alkaline phosphatase substrate or ^{125}I-protein A as previously described (26), except that Tris-buffered saline was substituted for phosphate-buffered saline. The anti-GCD11 antibodies were used at a 1:400 or 1:500 dilution and were obtained from a single rabbit (EH6) after a second boost with the *trpE-gcd11Δ106-273* fusion protein.

Analysis of rabbit eIF-2γ peptides. eIF-2 was purified from rabbit reticulocytes to fraction C by the method of Grifo et al. (21) and further purified on Sephadex G-75, DEAE-cellulose, and phosphocellulose (44). Purified eIF-2 was lyophilized to dryness and resuspended in 100 μl of formic acid. The sample was applied to a Beckman C-18 reverse-phase column (4.6 by 250 mm, 5-μm particle size) and equilibrated with 0.05% trifluoroacetic acid at a flow rate of

0.5 ml/min. Subunits were eluted from the column with a gradient from 0 to 75% acetonitrile over a period of 180 min. Fractions were monitored for A_{220} and A_{255}. Subunits were identified by SDS-polyacrylamide gel electrophoresis of lyophilized column samples resuspended in SDS sample buffer. The subunits were eluted with acetonitrile in the following order: β (38%), α (42%), and γ (48%). The β subunit was obtained in greater than 95% purity, and both the α and γ subunits were obtained in 80 to 90% purity. The α subunit was the major contaminant in the γ subunit preparation, at a level of 5 to 20%, depending upon the experiment.

For cyanogen bromide cleavage, a 100-μg aliquot of eIF-2γ was lyophilized to dryness and dissolved in a small volume of 100% formic acid. The sample was diluted to 70% formic acid with distilled water, and a 100-fold excess of cyanogen bromide-protein was added. The mixture was incubated overnight at room temperature in the dark. The digested sample was diluted with 5 volumes of water and lyophilized. The dried material was resuspended in 5 volumes of water and again lyophilized to dryness. A second 100-μg aliquot of eIF-2 was lyophilized to dryness and resuspended in 1 ml of 100 mM NH_4HCO_3 (pH 7.5). Tolylsulfonyl phenylalanyl chloromethyl ketone-treated trypsin (Cooper Biomedical) was added at a ratio of 1:100 and incubated at 37°C for 4 h. A second (equal) aliquot of tolylsulfonyl phenylalanyl chloromethyl ketone-treated trypsin was then added, and incubation was continued at 37°C overnight. The digested sample was lyophilized to dryness.

Samples were taken up in 200 μl of formic acid, diluted to 20% formic acid with water, and applied to a Beckman C-18 Ultrasphere ODS column (tryptic fragments) or a Synchrom C-8 SynChropak RP-P column (cyanogen bromide fragments) equilibrated with 0.05% trifluoroacetic acid at 1 ml/min. Peptides were eluted from the columns with a linear gradient of acetonitrile into 0.05% trifluoroacetic acid (0 to 60% in 3 h). A_{220} and A_{255} were monitored. Peptides to be sequenced were spotted onto Biobrene plus-treated glass fiber filters and analyzed by using an Applied Biosystems model 477A protein microsequencer (Molecular Biology Core Laboratory, Case Western Reserve University). The intact γ subunit was sequenced following SDS-polyacrylamide gel electrophoresis, transfer to Immobilon, and excision of the stained band for direct sequencing as described by Matsudaira (47).

Purification of yeast eIF-2. Yeast eIF-2 was purified from strain H1402 by using a modification (10a) of a published procedure (18). eIF-2 was partially purified from yeast strains harboring high-copy-number *SUI2*, *SUI3*, and/or *GCD11* plasmids by heparin-Sepharose fractionation of high-salt-washed crude extracts. GTP-dependent [^{3}H]Met-tRNA$_i$ (L-[methyl-^{3}H]methionine, 80 Ci/mmol; Amersham Corporation) binding was determined as described previously (18). Typical specific activity of [^{3}H]methionyl-tRNA was 92,500 dpm/μg of total tRNA.

Nucleotide sequence accession number. The nucleotide sequence data reported have been submitted to GenBank nucleotide sequence data bases under accession number L04268.

RESULTS

Isolation of the yeast *GCD11* gene. We isolated the wild-type *GCD11* gene from a yeast genomic library, constructed in the low-copy-number, centromere-containing plasmid YCp50 (58), by complementation of the growth defect present in the *gcn2-101 gcn3-101 gcd11-508* strain EY250. Preliminary experiments indicated that the YCp50-*GCN3* plasmid Ep69 partially alleviated the growth defect in EY250. However, the Ep69 transformants remained AT^r because the *gcd11* mutation suppresses the *gcn2* mutation present in this strain. We distinguished transformants bearing *GCN3* from those containing *GCD11* by the ability of the *GCD11* gene to complement the *gcd11* mutation and allow expression of the AT^s phenotype because of the *gcn* mutations in EY250.

From among 18,000 transformants of EY250, we obtained 10 in which complementation of the growth defect was plasmid dependent. This was demonstrated by plasmid-loss experiments in which transformants subjected to two cycles of growth on 5-FOA (FOA is toxic to URA3$^+$ strains [5]) regained the slow-growth phenotype of the untransformed parent. In addition, plasmids from these 10 transformants were rescued in *E. coli* and shown to complement the growth defect in EY250 when reintroduced into this strain. Four of the 10 plasmids isolated in this manner contained genomic clones of *GCN3*. The remaining six plasmids appeared to contain identical 4.5-kb inserts and were candidates for clones containing the *GCD11* gene. One of these plasmids, Ep264, was characterized further.

We determined if the 4.5-kb insert in Ep264 contained the *GCD11* gene by asking whether sequences within the insert could target integration of a plasmid to the *GCD11* locus. Plasmid Ep274 contains the 4.3-kb *Bam*HI-*Bgl*II genomic fragment (Fig. 1) from Ep264 inserted at the *Bam*HI site of the *LEU2*-containing yeast integrating plasmid YIp32. Ep274 was linearized at a unique *Sna*BI site located within the genomic insert and introduced into the *GCD11 gcn3-101 leu2-3,112* strain EY307. Southern blot analysis was used to confirm the directed integration of Ep274 in the Leu$^+$ transformants. One such transformant (EY424) was mated with the *gcd11-508 gcn3-101 leu2,3,112* strain EY252, and the diploids were sporulated and subjected to tetrad analysis. As expected, we observed 2:2 segregation for large and small colonies due to the *gcd11* mutation in EY252. In 24 of 24 complete tetrads, all large colonies were AT^s (*GCD11 gcn3*) and Leu$^+$, and all small colonies were AT^r (*gcd11-508 gcn3*) and Leu$^-$. These results indicated that *LEU2* was now linked to the wild-type *GCD11* allele. We conclude that the genomic fragment present in Ep274 contains the *GCD11* gene or, alternatively, sequences tightly linked to *GCD11*.

The *GCD11* complementation unit is coincident with a single, long ORF. The *GCD11* complementation unit was localized to a 2.1-kb *Hin*dIII-*Sna*BI restriction fragment by subcloning restriction fragments derived from the genomic insert in Ep264 into YCp50 and testing the resulting plasmids for their ability to complement a *gcd11* mutation (Fig. 1). Deletion analysis identified a similar 2.0-kb complementation unit bounded by the endpoints 5′Δ −104 and 3′Δ +1898. Plasmids containing unidirectional deletions used for deletion analysis were constructed by the method of Henikoff (29), starting with plasmids Ep359 and Ep360, which complement a *gcd11* defect.

Sequence analysis of the *GCD11* region revealed the presence of a single, long ORF of 527 codons (predicted molecular mass, 57,865 Da) extending from an ATG triplet at nucleotide +66 to a TAA termination codon at +1647 (Fig. 2). All 5′ deletion alleles that complemented a *gcd11* mutation include the +1 nucleotide, which corresponds to the transcription start site located farthest upstream (see below). 5′ deletion alleles lacking a portion of the long ORF failed to complement a *gcd11* mutation. The smallest 3′ deletion allele

that complemented a *gcd11* mutation (3′Δ +1898) includes the *Sna*BI restriction site at +1876 and appears to contain the complete *GCD11* transcription unit (see below). Removal of additional sequences in 3′Δ +1730 and 3′Δ +1676 gave rise to deletion alleles that weakly complemented a *gcd11* defect. These alleles lack sequences from the 3′ end of the *GCD11* transcription unit and may, therefore, give rise to *GCD11* transcripts with decreased stability. Further 3′ deletions that remove a portion of the *GCD11* ORF (e.g., 3′Δ +1310) failed to complement a *gcd11* mutation. The sequenced portion of the *GCD11* locus also contains a histidyl-tRNA gene (+2172 to +2243) with a predicted GUG anticodon represented by GTG at positions 2205 to 2207. The tRNA portion of this sequence is identical to three yeast His-tRNA clones described previously (14).

The following data confirmed that the putative *GCD11* ORF is required for complementation of a *gcd11* mutation. Ep510 is a low-copy-number plasmid containing the divergent *GAL1-GAL10* promoter fused to *GCD11* sequences at nucleotide +63 and extending to the *Sna*BI site at +1878. When introduced into the Gal$^+$ *gcd11* strain EY563, Ep510 complemented the growth defect in this strain when grown on galactose-containing media but not on glucose media. Ep509 is identical to Ep510 in sequence, but the orientation of the *GCD11* sequences is reversed. Ep509 failed to complement the growth defect in EY563 when the appropriate transformants were tested on either galactose or glucose media. Plasmid Ep433 contains the 2.1-kb *Hin*dIII-*Sna*BI *GCD11* fragment in the low-copy-number (in yeast cells) vector pRS316 and complemented a *gcd11* mutation. Removal of the 0.5-kb *Kpn*I fragment (Fig. 2; +380 to +884) from the *GCD11* sequences in Ep433 gave rise to a plasmid containing the *gcd11Δ106-273* allele that failed to complement a *gcd11* mutation. Finally, we constructed a derivative of Ep433 in which the plasmid was cleaved at the +884 *Kpn*I site, the overhanging 3′ ends were removed, and the plasmid was religated. This resulted in a 4-bp deletion within the putative *GCD11* ORF and gave rise to a deletion and frameshift allele that failed to complement a *gcd11* mutation. Taken together, these data indicate that the 527-codon ORF is required for *GCD11* function and encodes a polypeptide that is the product of the *GCD11* gene.

***GCD11* is an essential gene.** The genetic data (27, 28) suggested that at least some of the *gcd11* alleles encoded partially functional gene products. It was, therefore, of interest to determine the *gcd11* null phenotype. We constructed a deletion and insertion allele of *GCD11* [*gcd11*::*URA3* (*Δ1-527*)] by replacing the 2.1-kb *Hin*dIII-*Sna*BI *GCD11* fragment with a 1.1-kb fragment containing the yeast *URA3* gene (Fig. 3A). This deletion removes all *GCD11* coding sequences, along with 240 and 232 bp of the 5′ and 3′ flanking sequences, respectively. A 1.9-kb *Cla*I-*Pvu*II fragment containing the *gcd11*::*URA3* (*Δ1-527*) allele was introduced into a homozygous *GCD11 ura3-52 leu2-3,112* diploid strain (H4 × H1402). DNA was isolated from Ura$^+$ transformants, digested with *Eco*RI, and analyzed by Southern blot analysis with a *GCD11* probe. The probe used for experiments described in Fig. 3B hybridized with an 8.6-kb *Eco*RI fragment in *GCD11* strains. An additional 7.6-kb *Eco*RI fragment was detected in diploid strains in which one of the two *GCD11* alleles had been replaced by *gcd11*::*URA3* (*Δ1-527*). Diploid strains containing a single functional *GCD11* allele showed no apparent growth defect at 23°C. When *GCD11/gcd11*::*URA3* (*Δ1-527*) diploids were sporulated and dissected (Fig. 3C), two of four spores were viable in 37 of 38 four-spore tetrads (1 of 4 viability in a single tetrad). All viable spore clones were Ura$^-$, suggesting that the *gcd11*::*URA3* (*Δ1-527*) deletion allele is lethal. Microscopic examination of dissection plates incubated for 12 days at 23°C revealed that the inviable spores had failed to germinate.

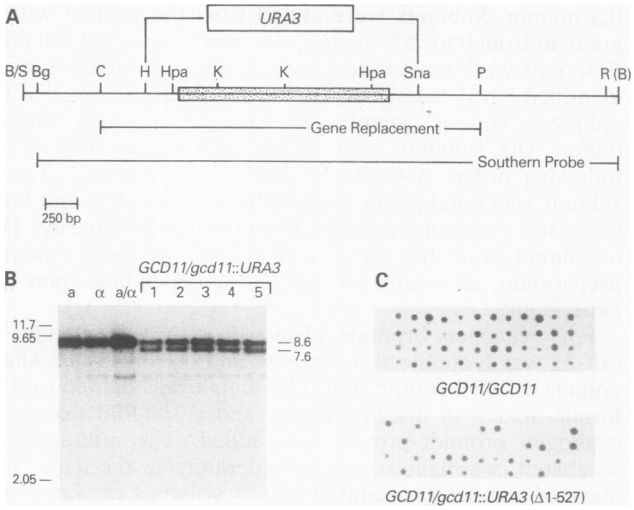

FIG. 3. Analysis of a *gcd11* deletion allele. (A) Partial restriction map of the *GCD11* fragment cloned in Ep264 as in Fig. 1. The 2.1-kb *Hin*dIII-*Sna*BI *GCD11* fragment was replaced with a 1.1-kb fragment containing the yeast *URA3* gene. The 1.9-kb *Cla*I-*Pvu*II fragment was used in gene replacement experiments to transform a homozygous *ura3-52* diploid strain (H4 × H1402) to Ura$^+$. (B) DNA was extracted from Ura$^+$ transformants of the diploid strain H4 × H1402 and digested with *Eco*RI. Restriction fragments were separated on a 1% agarose gel, transferred to nitrocellulose paper, and hybridized with a ^{32}P-labeled *Bam*HI-*Bgl*II *GCD11* restriction fragment shown in panel A. Lane a, strain H4; lane α, strain H1402; lane a/α, H4 × H1402 diploid; lanes 1 to 5, independent Ura$^+$ transformants of H4 × H1402. The sizes of molecular size markers (in kilobases) are shown to the left. Shown to the right are the sizes of genomic *Eco*RI fragments derived from the wild-type (8.6-kb) and the *gcd11*::*URA3* (*Δ1-527*) (7.6-kb) alleles. (C) H4 × H1402 (*GCD11/GCD11*) or H4 × H1402 [*GCD11/gcd11*::*URA3* (*Δ1-527*)] diploids were sporulated, dissected on YEPD media, and then incubated for 4 days at 23°C.

Although these results suggest that *GCD11* is an essential gene, it was possible that *GCD11* is required for germination only. To rule out this possibility, we introduced plasmid Ep415, a low-copy-number *LEU2* plasmid that contains the 2.1-kb *Hin*dIII-*Sna*BI *GCD11* fragment, into the *GCD11/gcd11*::*URA3* (*Δ1-527*) diploid strain constructed above. Leu$^+$ diploid transformants were sporulated and subjected to tetrad analysis. We observed tetrads with four (eight tetrads), three (six tetrads), and two (nine tetrads) viable spores, in contrast to a transformant of the *GCD11/gcd11*::*URA3* (*Δ1-527*) diploid containing the vector alone, which gave rise to tetrads containing only two viable spores. In the case of the Ep415 transformants, all of the Ura$^+$ [*gcd11*::*URA3* (*Δ1-527*)] spore clones were also Leu$^+$, indicating that they harbored Ep415. We chose two tetrads that showed 2 Ura$^+$ Leu$^+$: 2 Ura$^-$ Leu$^+$ segregation and passaged cells derived from each spore clone under nonselective conditions. After approximately 40 generations, all cells derived from the Ura$^+$ Leu$^+$ spore clones remained Leu$^+$, while 60 to 80% of the cells derived from the original Ura$^-$ Leu$^+$ spore clones were now Leu$^-$. This suggests that cells containing the *gcd11* null allele must retain Ep415 for viabil-

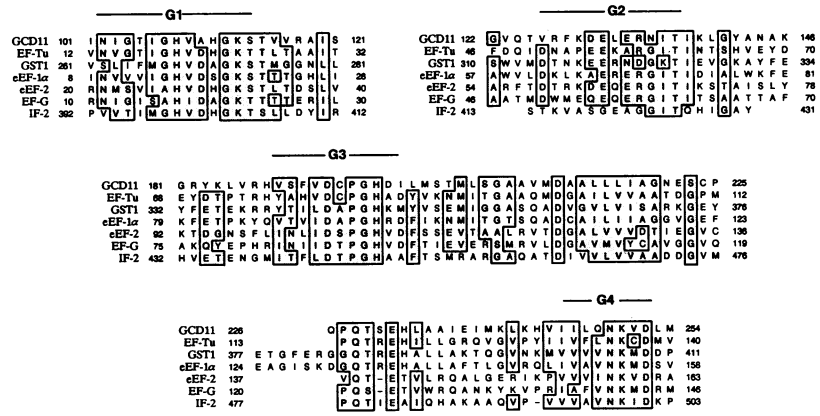

FIG. 4. Alignment of G1 to G4 regions (8) present in GTP-binding translational factors with the predicted GCD11 polypeptide. Shaded regions contain residues that are either identical or conserved in at least five of the sequences, according to the following Dayhoff (13, 20) categories: A, G, P, S, and T; I, M, L, and V; F, W, and Y; C; D, E, N, and Q; H, K, and R. The sequences aligned with GCD11 are *E. coli* EF-Tu (2, 37, 72); *S. cerevisiae* GST1 (an eEF-1α homolog [38]), eEF-1α (12, 50, 62), and eEF-2 (55); and *E. coli* EF-G (52, 56) and IF-2 (60).

ity. These results and the data presented above demonstrate that *GCD11* is an essential gene in *S. cerevisiae*.

The predicted GCD11 polypeptide is similar to EF-Tu and other GTP-binding translational factors. Computer-assisted searches of published data bases revealed striking similarity between the predicted GCD11 polypeptide and GTP-binding translational factors, including the prokaryotic elongation factor EF-Tu, eukaryotic elongation factors eEF-1α and eEF-2, and the prokaryotic initiation factor IF2 (Fig. 4). The highest similarity scores were obtained in comparing GCD11 with bacterial and yeast mitochondrial EF-Tu, a factor that forms a complex with GTP and aminoacylated elongating tRNAs. The similarity between GCD11 and EF-Tu begins at residue 91 in GCD11, corresponding to the amino terminus of the mature *E. coli* EF-Tu protein. The 90-amino-acid N-terminal extension predicted by the *GCD11* sequence is highly charged (33 of 90 residues), containing 24 acidic and 9 basic residues. Relative to EF-Tu, amino-terminal extensions of various lengths are also present in the prokaryotic initiation factor IF2 and the eEF-1α homolog GST1. In the case of IF2, these N-terminal sequences appear to be dispensable for function (for a review, see reference 22).

The greatest degree of similarity between GCD11 and the family of GTP-binding translational factors occurs in the regions labeled G1 through G4 in Fig. 4. These regions contain residues involved in GTP-binding and hydrolysis, whose primary sequence and spacing are conserved in all GTP-binding translational factors and are present in the predicted GCD11 polypeptide. Regions G1 (G-X_4-G-K-S/T), G2, and G3 (D-X-X-G) interact with the phosphate groups of bound GTP or GDP. Region G4 (N-K-X-D) interacts with the purine ring of bound guanine nucleotides (for a review, see reference 8).

Additional features of the predicted GCD11 polypeptide include a consensus cyclic AMP-dependent protein kinase phosphorylation site at a threonine residue at position 521 and a cysteine-rich region extending from residues 155 to 179 that bears primary sequence similarities to metal-binding finger structures of the Cys-X_4-Cys type (4). Two amino terminus-proximal Cys-X_4-Cys sequences are present at residues 150 to 155 and 155 to 160. We do not yet know the significance of these sequence motifs.

The predicted GCD11 polypeptide contains sequences similar to rabbit and porcine eIF-2γ peptides. The combined sequence and genetic data suggest that *GCD11* encodes a GTP-binding protein involved in protein synthesis. A number of GTP-binding translational factors have been characterized in eukaryotic organisms. These include the initiation factor eIF-2 and the elongation factors eEF-1α and eEF-2. Duplicate genes encoding eEF-1α (*TEF-1* and *TEF-2* [12, 50, 62]) and eEF-2 (*EFT1* and *EFT2* [55]) have been cloned from yeasts, and their predicted amino acid sequences are not identical to the deduced GCD11 sequence. The amino acid sequence predicted by the yeast *SUP2* gene (also called *SUF12* and *GST1* [38, 42]), which encodes an eEF-1α homolog, is also similar but not identical to that predicted by the *GCD11* sequence.

eIF-2 is a complex composed of three nonidentical subunits termed α (36 kDa), β (38 kDa), and γ (55 kDa). eIF-2 binds GTP and charged Met-$tRNA_i$ to form a ternary complex that functions in the initiation of protein synthesis in eukaryotic organisms. The yeast *SUI2* and *SUI3* genes, which encode the α and β subunits of eIF-2, respectively, have been cloned and sequenced (11, 18). *SUI2* and *SUI3* are essential genes that are present in single copy in haploid yeast cells. Mutations in *SUI2* and *SUI3* confer phenotypes similar to those conferred by known *gcd11* alleles: growth defect, constitutive derepression of the general control, and suppression of loss of function mutations in *GCN2* and *GCN3* (69). The deduced amino acid sequences for the yeast α and β subunits lack consensus elements found in GTP-binding proteins. Therefore, we considered it possible that *GCD11* is the structural gene for yeast eIF-2γ.

Comparison of published amino acid sequence data for eIF-2γ peptides with the deduced GCD11 sequence revealed blocks of sequences similar to the γ 1, 2a, 2b, 3b, 4a, and 6 peptides determined by Suzuki et al. (67) for porcine eIF-2γ and the fragment 1 and 2 peptides determined by Bommer et al. (6) for rabbit eIF-2γ. These peptides are aligned with the deduced GCD11 amino acid sequence in Fig. 5. We have extended these sequence similarities by determining the amino acid sequence of additional peptides derived from rabbit eIF-2γ. Peptides were obtained by treatment of purified γ subunit with either cyanogen bromide or trypsin. The sequenced peptides are listed in Table 2 and are aligned with the deduced GCD11 polypeptide in Fig. 5.

Peptides designated CB-108 and CB-82B in Table 2 overlap with fragments 1 and 2, respectively, of Bommer et al. (6)

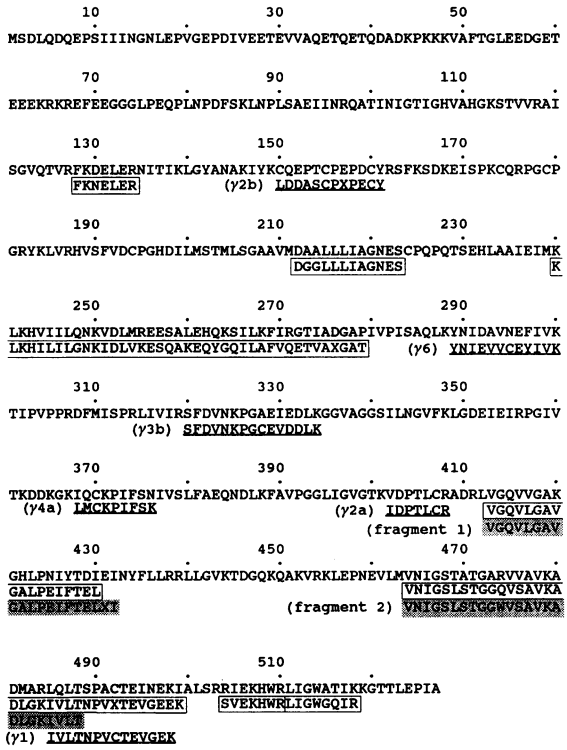

FIG. 5. Alignment of the rabbit and porcine eIF-2γ peptides (lower sequences) with the predicted GCD11 amino acid sequence (upper sequence). Underlined peptides were determined by Suzuki et al. (67) for porcine eIF-2γ; shaded peptides were determined by Bommer et al. (6) for rabbit eIF-2γ; boxed peptides are those reported in this paper (see also Table 2). Single-letter amino acid codes are used, with X indicating uncertainty in determining the amino acid at that position.

(Fig. 5). The regions of overlap are identical, except at deduced residue arginine 474 of the yeast GCD11 sequence, which has been determined to be a glutamine residue (this work) and a tryptophan residue (6) in rabbit eIF-2γ. We do not find a reasonable match with the γ3a peptide of Suzuki et al. (67), nor can we unambiguously assign a match with peptides T2-51, T2-60B, T2-74B, and CB-78A in Table 2. A peptide similar to the consensus amino-terminal peptide AGGEAGVT(G/L)G(E/Q)(S/P) (CB-82A [6 and references cited therein]) of rabbit eIF-2γ is also absent from the GCD11 sequence. Overall, we have aligned 182 amino acid residues (not including residues denoted by X [Fig. 5]) determined for rabbit and porcine eIF-2γ, in peptides ranging from 7 to 39 residues, to sequences within the predicted 527 amino acids of the GCD11 sequence. Comparison of the GCD11 sequence and the combined rabbit and porcine sequences in Fig. 5 shows 64% identical residues.

Cooverexpression of SUI2, SUI3, and GCD11 leads to increased eIF-2 activity. Yeast strains harboring a high-copy-number plasmid containing either the *SUI2*, *SUI3*, or *GCD11* gene contain elevated steady-state levels of the corresponding gene product (11, 18; this work). If GCD11 is eIF-2γ, extracts prepared from yeast strains cooverexpressing all three eIF-2 subunits might be expected to exhibit increased eIF-2 activity. To test this idea, we constructed a set of isogenic strains harboring multicopy plasmids that overexpressed either *GCD11*, *SUI2* and *SUI3*, or *SUI2*, *SUI3*, and *GCD11*. eIF-2 was partially purified by heparin-Sepharose chromatography of high-salt-washed extracts prepared from each strain. eIF-2 activity was measured as GTP-dependent binding of Met-tRNA$_i$ (ternary complex formation). Strains harboring the high-copy-number *GCD11* plasmid or the high-copy-number *SUI2* plus *SUI3* plasmid show levels of ternary complex activity (0.02 and 0.03 pmol of [^{3}H]Met-tRNA$_i$ bound per μg of protein) similar to that of the wild-type parent harboring the high-copy-number vectors alone (0.03 pmol/μg of protein). Significantly, extracts prepared from a strain harboring *SUI2*, *SUI3*, and *GCD11* in high copy show a four- to fivefold increase in the level of ternary complex formation activity (0.13 pmol/μg of protein).

Anti-GCD11 antibodies cross-react with the γ subunit of purified yeast eIF-2. We utilized polyclonal rabbit antibodies raised against a *trpE-GCD11* fusion protein as a probe to detect GCD11 protein in yeast cell extracts. The specificity of the anti-trpE-GCD11 antibodies for the authentic yeast GCD11 protein was demonstrated by using extracts prepared from yeast strains harboring different *GCD11* alleles. The first two lanes in Fig. 6 contain equivalent amounts of protein extracted from the wild-type strain H1402 harboring either a high-copy-number *GCD11*-containing plasmid (lane h.c. *GCD11*) or the high-copy-number vector alone (lane s.c. *GCD11*). The antibodies cross-react with a 58-kDa polypeptide in extracts prepared from the single-copy *GCD11* strain whose abundance is increased in H1402 harboring the high-copy-number *GCD11* plasmid. Extracts were also prepared

TABLE 2. Sequenced peptides from rabbit eIF-2γ

Peptide	Digest	Sequence
T2-96	Trypsin	LIGWGQIR
T2-64	Trypsin	FKNELER
T2-51	Trypsin	GVITIKPTVR
T2-60A	Trypsin	HWR
T2-60B	Trypsin	DFTSER
T2-74A	Trypsin	SVEKHWR
T2-74B	Trypsin	LDEPR
T2-86	Trypsin	IVLTNPVSTEVGEEK
CB-82A	CNBr	AGGEAGVTGGE(S/P)F
CB-82B	CNBr	VNIGSLSTGGQVSAVKADLGKIVLTNPV(H/S)TEVGEEK
CB-78A	CNBr	LNIGSLIALNQ
CB-82D	CNBr	DGGLLLIAGNES
CB-100	CNBr	KLKHILILGNKIDLVKESQAKEQYGQILAFVQETVA(E/Y)GAT
CB-108	CNBr	VGQVLGAVGALPEIFTEL

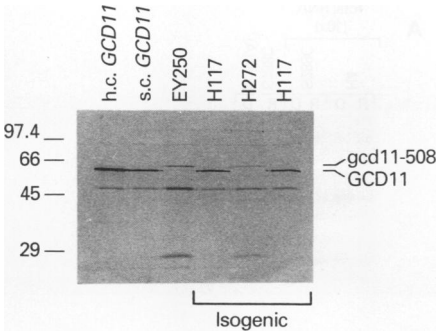

FIG. 6. Specificity of anti-GCD11 antiserum. Total protein extracts were prepared from the indicated strains, fractionated by SDS-polyacrylamide gel electrophoresis, and analyzed by Western blot analysis with anti-GCD11 antiserum (1:400). Strains were grown in supplemented minimal medium. Lane h.c. *GCD11*, strain H1402 harboring the high-copy-number plasmid Ep361 (YEp24-*GCD11*); lane s.c. *GCD11*, strain H1402 harboring YEp24. EY250 is the *gcd11-508* strain used in the isolation of the *GCD11* gene. H272 contains the *gcd11-508* allele and was isolated as an AT^r revertant of the *gcn2-101 gcn3-101 GCD11* strain H117 (28). This blot was developed by using alkaline phosphatase-conjugated goat anti-rabbit immunoglobulin G and a 5-bromo-4-chloro-3-indolylphosphate toluidinium–nitroblue tetrazolium color development system (Bio-Rad). The mobilities of the wild-type GCD11 protein and the polypeptide encoded by the *gcd11-508* allele are indicated to the right. Numbers to the left indicate the mobilities of the following protein molecular mass markers (Sigma SDS-6H): phosphorylase B (97.4 kDa), bovine serum albumin (66 kDa), ovalbumin (45 kDa), and carbonic anhydrase (29 kDa).

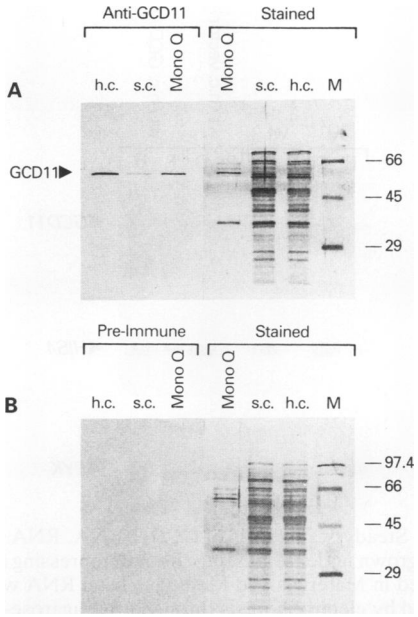

FIG. 7. Anti-GCD11 antibodies cross-react with yeast eIF-2γ. Protein samples were denatured and fractionated on SDS–10% polyacrylamide gels and transferred to nitrocellulose. (A) Duplicate samples were separated on a single gel and transferred to nitrocellulose paper, which was subsequently divided in half. The left half was incubated with anti-GCD11 antisera (1:500 dilution) and developed by using alkaline phosphatase-conjugated secondary antibody and substrate as described in the legend to Fig. 6. This blot was overdeveloped in order to visualize GCD11 in the extract prepared from the single-copy *GCD11* strain (lane s.c. *GCD11*). Proteins in the duplicate samples on the right half were stained with colloidal gold (Bio-Rad). (B) As in panel A, except the left half was incubated with a 1:500 dilution of preimmune sera. Lanes h.c. and s.c. contain extracts from the same high-copy-number *GCD11* and single-copy *GCD11* strains used in Fig. 6; lanes Mono Q contain a fraction (100 ng of total protein) enriched for ternary complex formation activity obtained by chromatography on a Mono Q (Pharmacia) column; lane M, protein markers used as molecular mass standards are the same as in Fig. 6.

from strain EY250 (*gcd11-508*) and the isogenic strains H117 (*GCD11*) and H272 (*gcd11-508*). The *gcd11-508* mutation is the result of the insertion of a Ty element into C-terminal *GCD11* coding sequences that extends the *GCD11* ORF by 30 codons (18a). The anti-GCD11 antibodies did not detect a protein species corresponding to the wild-type GCD11 protein in extracts prepared from either *gcd11-508* strain but, rather, detected a polypeptide with decreased mobility consistent with the molecular nature of the *gcd11-508* mutation.

We tested for cross-reactivity of the anti-GCD11 antibodies with polypeptides present in eIF-2 purified from a wild-type yeast strain. Immunoblot analyses with antisera against eIF-2α and eIF-2β and the activity of eIF-2 in ternary complex formation assays with GTP and $[^3H]$Met-$tRNA_i$ were used to follow the purification of yeast eIF-2. The peak fraction of ternary complex formation activity was taken from a Mono Q column used in the final purification step and analyzed by SDS-polyacrylamide gel electrophoresis. Duplicate samples were denatured and fractionated on a single gel and transferred to nitrocellulose paper (Fig. 7). One half of the paper was stained for total protein and the other half was probed with anti-GCD11 antibodies (panel A) or with preimmune serum (panel B).

Two major polypeptides, 36 and 58 kDa, were detected by staining the yeast eIF-2 sample obtained from the Mono Q column. The 36-kDa species is a doublet band consisting of eIF-2α and eIF-2β polypeptides that are not resolved in this gel system (11, 18). The size of the 58-kDa polypeptide in the stained blots is consistent with the molecular mass of mammalian eIF-2γ. This 58-kDa polypeptide comigrated with a 58-kDa polypeptide in the purified eIF-2 preparation that cross-reacted with anti-GCD11 antibodies and also with the GCD11 protein recognized in whole-cell extracts by anti-GCD11 antibodies. No cross-reactivity was detected when preimmune serum was used (Fig. 7B). Taken together, our data indicate that *GCD11* encodes a 58-kDa polypeptide that is the γ subunit of eIF-2 in *S. cerevisiae*.

The level of GCD11 mRNA is not regulated by amino acid availability. Results of RNA hybridization analyses (Northern blot) presented in Fig. 8 demonstrate that the level of the *GCD11* transcript is unaffected by amino acid availability. In two related wild-type strains, the steady-state levels of a ca. 1.9-kb transcript derived from the *GCD11* locus were similar in unstarved (repressed) and starved (derepressed) cells. Wild-type strain H4 harboring a high-copy-number plasmid containing the *Hin*dIII-*Sna*BI *GCD11* fragment overproduced the *GCD11* transcript (lanes wt/h.c. *GCD11*) compared with strain H4 harboring the YEp24 vector alone (lanes wt/h.c. vector). As expected, the level of the *HIS4* transcript increased 6- to 11-fold in response to amino acid starvation in wild-type cells. Interestingly, the *HIS4* transcript was elevated two- to threefold, when normalized for *PYK* mRNA, in strains overproducing *GCD11* mRNA under repressed growth conditions. This result is consistent with our observations (unpublished) that overexpression of *GCD11* leads to partial derepression of the general control. This effect of overexpression of *GCD11* may be due, in part,

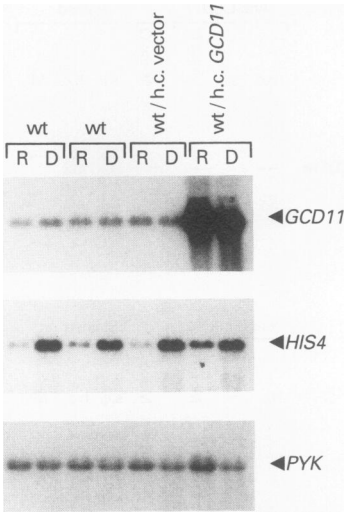

FIG. 8. Steady-state levels of *GCD11* RNA. RNA was extracted from cells grown under repressing (R) or derepressing (D) conditions as described in Materials and Methods. Total RNA was denatured, fractionated by electrophoresis through a 1% agarose-formaldehyde gel, and then transferred to a GeneScreen Plus (New England Nuclear) membrane and hybridized with a ^{32}P-labeled probe as indicated. The *GCD11* probe was the 2.1-kb *Hin*dIII-*Sna*BI *GCD11* fragment. Blots hybridized with *GCD11* and *HIS4* probes were prepared from separate gels. The blot hybridized with the *GCD11* probe was stripped according to the manufacturer's protocol and rehybridized with the *PYK* probe. Lanes wt, *GCD11* strains H4 and H1402 (left to right); lanes wt/h.c. vector, strain H4 harboring the multicopy autonomous yeast vector YEp24; lanes wt/h.c. *GCD11*, strain H4 harboring Ep361 (YEp24-*GCD11*).

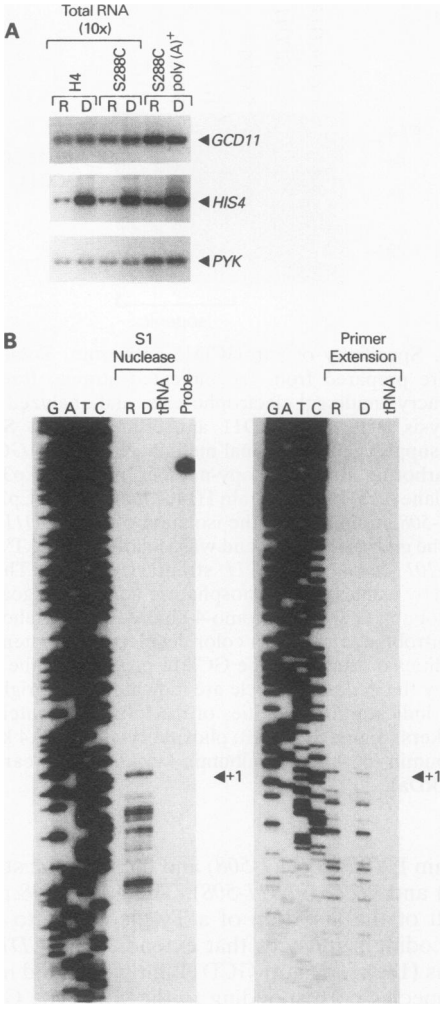

FIG. 9. Mapping the 5′ end of *GCD11* mRNA. The indicated *GCD11* strains were grown under repressing (R) and derepressing (D) conditions as described in Materials and Methods. (A) Total and poly(A)$^+$-enriched RNAs were analyzed by blot hybridization analysis as described in the legend to Fig. 8. Total RNA lanes (lanes H4 and S288C) contain approximately 10-fold-more RNA than the lanes containing poly(A)$^+$ RNA [lanes S288C, poly(A)$^+$]. (B) The 5′ end of *GCD11* mRNA was determined by using poly(A)$^+$ RNA prepared from strain S288C. For S1 analysis, RNA was hybridized with a 5′-end-labeled +137 to −180 DNA probe, and the RNA-DNA hybrids were digested with S1 nuclease (200 U/ml). For primer extension analysis, a 5′-end-labeled +137 to +117 oligonucleotide primer was hybridized with poly(A)$^+$ RNA and extended with avian myeloblastosis virus reverse transcriptase. Protected DNA fragments (S1 Nuclease) and primer extension products (Primer Extension) were fractionated on polyacrylamide–8 M urea gels along with a sequencing ladder (lanes G, A, T, and C) prepared by using *GCD11* sequences as a template and the +137 to +117 oligonucleotide as a primer. Lanes tRNA, tRNA control; lane Probe, 317-nucleotide probe used in S1 nuclease analysis.

to the formation of inactive complexes between eIF-2γ and other components involved in translation initiation that reduce the level of eIF-2 function in the cell. A 1.9-kb RNA species in the same relative amount was detected when either the 2.1-kb *Hin*dIII-*Sna*BI fragment or the 1.48-kb *Hpa*I-*Hpa*I (+43 to +1525) *GCD11* fragment was used as a probe, indicating that the RNA species observed is derived from sequences containing the *GCD11* ORF.

Data presented in Fig. 9A demonstrate that the *GCD11* transcript is enriched by about 20-fold in a poly(A)-containing RNA fraction obtained by a single passage of total RNA through an oligo(dT)-cellulose column. This poly(A)-enriched RNA was used for S1 nuclease and primer extension mapping experiments to determine the 5′ end of the *GCD11* mRNA. The results shown in Fig. 9B indicate the presence of multiple transcription start sites. However, only those start sites at positions +1, +12, and +35 were detected by both methods. In addition, all putative transcription start sites were represented in the same relative proportions in RNA prepared from repressed and derepressed cells. The longest 5′ leader was 72 nucleotides in length and is devoid of upstream ORFs. Low-resolution experiments to determine the 3′ end of the *GCD11* transcript suggest that the transcript ends 10 to 20 nucleotides from the *Sna*BI site (+1878) in both repressed and derepressed cells (data not shown). This is consistent with both the size (ca. 1.9 kb) of the *GCD11* transcript, as determined by Northern blot analysis, and 5′ end mapping data. In addition, haploid strains bearing deletions of the *GCD11* locus but harboring a low-copy-number plasmid containing the *Hin*dIII-*Sna*BI *GCD11* fragment contained a *GCD11* transcript that comigrated on Northern blots with the wild-type *GCD11* transcript (data not shown). We conclude that *GCD11* is transcribed into a polyadenylated RNA whose size and abundance are unaffected by amino acid availability in *S. cerevisiae*.

Steady-state levels of GCD11 protein remain constant in unstarved and amino acid-starved cells. Anti-GCD11 antibod-

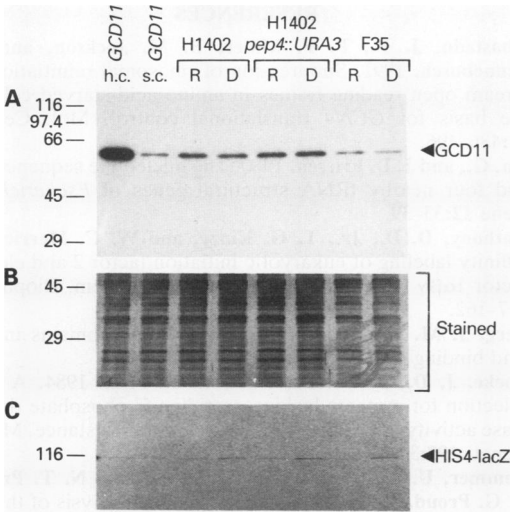

FIG. 10. Steady-state levels of GCD11. Total protein was extracted from the indicated strains grown under repressing (R) or derepressing (D) conditions as described in Materials and Methods. Protein samples were denatured, fractionated on SDS-polyacrylamide gels, and electrophoretically transferred to nitrocellulose paper. (A) Transferred proteins were incubated with a 1:500 dilution of anti-GCD11 antiserum. The blot was then washed, and bound antibodies were detected by incubating the blot with ^{125}I-protein A, washing, and exposure to X-ray film. (B) Transferred proteins were stained with colloidal gold total protein stain. (C) Transferred proteins were incubated with a mouse monoclonal anti-β-galactosidase antibody (Promega) to detect the *HIS4-lacZ* fusion protein present in these strains. The blot in panel C was developed as in Fig. 6, except alkaline phosphatase-conjugated goat anti-mouse immunoglobulin G was used. Lanes h.c. *GCD11* and s.c. *GCD11* contain extracts from the same high-copy-number and single-copy *GCD11* strains used in Fig. 6. Strains H1402, H1402 *pep4::URA3* (EY482; isogenic with H1402), and F35 carry the wild-type *GCD11* allele. Numbers to the left indicate the mobilities (in kilodaltons) of the same molecular mass markers used in Fig. 6. The 116-kDa marker protein is β-galactosidase.

ies were used as a probe to compare steady-state levels of GCD11 in extracts prepared from unstarved and starved cells. Lanes h.c. *GCD11* and s.c. *GCD11* in Fig. 10 contain equivalent amounts of protein in extracts prepared from high-copy-number *GCD11* and single-copy *GCD11* H1402 derivatives. Extracts prepared from repressed and derepressed cultures of *GCD11* strains *H1402*, *H1402* (*pep4::URA3*), and F35 contain similar steady-state levels of GCD11 protein (Fig. 10A). In these same extracts, the level of a *HIS4-lacZ* fusion protein increases in response to amino acid starvation (Fig. 10C). Therefore, the derepression of general control-regulated genes, such as *HIS4*, that occurs in response to amino acid starvation is not accompanied by a change in the level of the GCD11 protein.

DISCUSSION

We have presented evidence that *GCD11* encodes the γ subunit of eIF-2 in *S. cerevisiae*. This conclusion is based upon three lines of evidence. First, peptides predicted by the *GCD11* nucleotide sequence are similar to peptide sequences, obtained by amino acid sequence analysis, present in rabbit and porcine eIF-2γ. We find that 64% of the amino acid residues are identical in a partial alignment between the yeast and combined rabbit and porcine sequences (Fig. 5). When conservative substitutions are also considered (by using the Dayhoff categories given in the legend to Fig. 4), the overall similarity is 83%. In comparison, the amino acid sequences predicted by the yeast and human genes encoding eIF-2α show 58% identical residues, while the predicted eIF-2β sequences indicate 42% identical residues (11, 18). Second, a 58-kDa polypeptide in highly purified preparations of yeast eIF-2 is recognized by antisera raised against the GCD11 polypeptide. This 58-kDa polypeptide comigrates on denaturing polyacrylamide gels with the GCD11 polypeptide, identified by GCD11-specific antisera, in whole-cell extracts. Finally, cooverexpression of GCD11, SUI2 (eIF-2α), and SUI3 (eIF-2β) leads to a four- to fivefold increase in the level of ternary complex formation activity present in yeast eIF-2 preparations. In contrast, cells overexpressing the α and β subunits of eIF-2 in the absence of extra copies of *GCD11* or overexpressing GCD11 alone give rise to eIF-2 preparations with wild-type levels of ternary complex formation activity.

Characterization of the yeast gene encoding the γ subunit of eIF-2 provides new information regarding guanine nucleotide binding by eIF-2. Previous experiments in which guanine nucleotide analogs were cross-linked to rabbit eIF-2 indicated that GTP-binding might be a shared function of the β and γ subunits (3, 6 [and references cited therein]). The presence of two putative GTP-binding elements (DXXG and NKXD) within the predicted human eIF-2β polypeptide (54) is consistent with the notion of shared binding. However, the fact that the predicted yeast eIF-2β polypeptide is devoid of consensus GTP-binding elements (18) and the unusually long distance (125 residues) between the two elements predicted by the human cDNA sequence argue against direct participation of the β subunit in guanine nucleotide binding. The amino acid sequence predicted by the *GCD11* gene contains all of the elements known to be required for guanine nucleotide binding (8) and suggests that the γ subunit of yeast eIF-2 is sufficient for GDP and GTP binding. This idea will be tested directly. In this view, the cross-linking experiments might indicate a close physical association between eIF-2β and the guanine nucleotide binding pocket formed by the γ subunit. However, the data do not rule out the possibility of a more direct interaction between eIF-2β and the guanine nucleotide.

Preliminary data indicate that it is possible to align the deduced GCD11 amino acid sequence within the structural model for EF-Tu (48a). Similar alignments based upon the EF-Tu model (40) have been proposed by using the deduced amino acid sequences of rabbit eEF-1α (39) and yeast eEF-2 (55). The implied functional similarities between EF-Tu and eIF-2γ suggest that the γ subunit of eIF-2 may also interact directly with initiator tRNA. On the basis of cross-linking studies, Kinzy et al. (39) have proposed that binding of aminoacylated-tRNA on eEF-1α involves close interactions between tRNA and domains II and III of the proposed eEF-1α structure. Their data place the anticodon loop of the tRNA molecule near the GTP-binding pocket (domain I) of eEF-1α. The analogous placement of the initiator tRNA anticodon loop near the guanine nucleotide binding site on eIF-2γ might serve to regulate initiator tRNA binding and/or facilitate the coupling of GTP hydrolysis to the recognition of the AUG start codon for protein synthesis. The latter is consistent with results of previous genetic analyses of yeast cells that indicate a role for both eIF-2 and Met-tRNA$_i^{Met}$ in AUG start codon recognition (9, 11, 18).

The amino acid sequence alignments presented in Fig. 4 pair threonine residue 137 in the G2 region of the GCD11

sequence with residue threonine 61 in the EF-Tu sequence. This threonine residue corresponds to threonine 35 of $p21^{ras}$, which is coordinated with a Mg^{2+} ion that is, in turn, coordinated with the β and γ phosphates in the $p21^{ras}$-GppNHp crystal structure (53). One potential outcome of the pairing in Fig. 4 is an increase in the size of a loop region (the L3 loop [53, 70]) that precedes the DXXG consensus element. Curiously, the additional GCD11 amino acids (residues 150 to 179) include the cysteine-rich region containing the putative finger motif. Alternative alignments in this region (data not shown) lead to differences in a region of the protein that corresponds to the L2 loop region in the $p21^{ras}$ crystal structure (53, 70) that is believed to interact with GTPase-activating molecules such as GAP (for a review, see references 8 and 70). Further refinements in the comparative molecular modeling of this region should aid in distinguishing between these possibilities.

Mutations in the yeast *GCD11* gene were originally isolated as suppressors of loss-of-function mutations in the yeast *GCN2* and *GCN3* genes (28). Both *GCN2* and *GCN3* are required for starvation-induced derepression of *GCN4* translation. *GCN2* encodes a protein kinase that phosphorylates the α subunit of eIF-2 in amino acid-starved cells (15). *GCN3* appears to encode a nonessential subunit of the guanine nucleotide exchange factor, eIF-2B, that catalyzes GDP-GTP exchange on eIF-2 (10). The suggested roles of *GCN2* and *GCN3* as positive effectors of general control is to reduce (antagonize) eIF-2 activity in amino acid-starved cells (15). Mutations in essential genes encoding subunits of eIF-2 (*SUI2*, *SUI3*, and *GCD11*) or eIF-2B (*GCD1* and *GCD2*) lead to constitutively elevated translation of *GCN4* coding sequences, presumably because the activity of these initiation factors is reduced in mutant strains in both unstarved and starved cells. Genetic evidence, in the form of allele-specific interactions between *GCD11* and *GCN3* (27), indicates that the effect of *GCN3* on the expression of the Gcd^- phenotype in *gcd11* strains may be mediated by protein-protein contact between GCN3 and eIF-2γ. In wild-type cells, this interaction appears to be critical for the increased translation of *GCN4* coding sequences that occurs under starvation conditions, since null alleles of *GCN3* confer a nonderepressible phenotype (24). Consistent with the important role of *GCN3* in the derepression response, constitutively activating alleles of *GCN2* require GCN3 for maximal derepression (26). It is possible that the absence of GCN3 reduces the ability of GCN2 to phosphorylate eIF-2α in vivo. Alternatively, GCN3 may act to enhance the stability of the complex formed between eIF-2B and an eIF-2–GDP binary complex phosphorylated at serine 51 on eIF-2α in starved cells. The isolation of the structural gene for the γ subunit of yeast eIF-2 will allow us to examine the proposed interactions between eIF-2γ and GCN3, as well as to further explore the role of the γ subunit of eIF-2 in the initiation of protein synthesis.

ACKNOWLEDGMENTS

We are indebted to Alan Hinnebusch (National Institutes of Health) and Bill Merrick (Case Western Reserve Medical School) for valuable comments on the manuscript, to Tom Dever and Tom Donahue for plasmids and antisera against yeast eIF-2α and eIF-2β, and to Alan Hinnebusch and Paul Miller for yeast strains. We thank The University of Texas Southwest Medical Center for the use of computer facilities.

T.G.K. was supported by National Institutes of Health grant GM26796 (to William C. Merrick). This work was supported by National Science Foundation grant DMB-9105892 to E.M.H.

REFERENCES

1. **Abastado, J. P., P. F. Miller, B. M. Jackson, and A. G. Hinnebusch.** 1991. Suppression of ribosomal reinitiation at upstream open reading frames in amino acid-starved cells forms the basis for *GCN4* translational control. Mol. Cell. Biol. **11**:486–496.
2. **An, G., and J. D. Friesen.** 1980. The nucleotide sequence of *tufB* and four nearby tRNA structural genes of *Escherichia coli*. Gene **12**:33–39.
3. **Anthony, D. D., Jr., T. G. Kinzy, and W. C. Merrick.** 1990. Affinity labeling of eukaryotic initiation factor 2 and elongation factor 1αβγ with GTP analogs. Arch. Biochem. Biophys. **281**: 157–162.
4. **Berg, J. M.** 1986. Potential metal-binding domains in nucleic acid binding proteins. Science **232**:485–487.
5. **Boeke, J. D., F. Lacroute, and G. R. Fink.** 1984. A positive selection for mutants lacking orotidine-5′-phosphate decarboxylase activity in yeast: 5-fluoro-orotic acid resistance. Mol. Gen. Genet. **197**:345–347.
6. **Bommer, U.-A., R. Kraft, T. V. Kurzchalia, N. T. Price, and C. G. Proud.** 1991. Amino acid sequence analysis of the β- and γ-subunits of eukaryotic initiation factor eIF-2. Identification of regions interacting with GTP. Biochim. Biophys. Acta **1079**: 308–315.
7. **Botstein, D., S. C. Falco, S. E. Stewart, M. Brennan, S. Scherer, D. T. Stinchcomb, K. Struhl, and R. W. Davis.** 1979. Sterile host yeasts (SHY): a eukaryotic system of biological containment for recombinant DNA experiments. Gene **8**:17–24.
8. **Bourne, H. R., D. A. Sanders, and F. McCormick.** 1991. The GTPase superfamily: conserved structure and molecular mechanism. Nature (London) **349**:117–127.
9. **Cigan, A. M., L. Feng, and T. F. Donahue.** 1988. $tRNA_i^{Met}$ functions in directing the scanning ribosome to the start site of translation. Science **242**:93–97.
10. **Cigan, A. M., M. Foiani, E. M. Hannig, and A. G. Hinnebusch.** 1991. Complex formation by positive and negative translational regulators of *GCN4*. Mol. Cell. Biol. **11**:3217–3228.

10a. **Cigan, A. M., and A. G. Hinnebusch.** Personal communication.

11. **Cigan, A. M., E. K. Pabich, L. Feng, and T. F. Donahue.** 1989. Yeast translation initiation suppressor *sui2* encodes the α subunit of eukaryotic initiation factor 2 and shares identity with the human α subunit. Proc. Natl. Acad. Sci. USA **86**:2784–2788.
12. **Cottrelle, P., D. Thiele, V. L. Price, S. Memet, J. Y. Micouin, C. Marck, J. M. Buhler, A. Sentenac, and P. Fromageot.** 1985. Cloning, nucleotide sequence, and expression of one of two genes coding for yeast elongation factor 1α. J. Biol. Chem. **260**:3090–3096.
13. **Dayhoff, M. O., R. M. Schwartz, and B. C. Orcutt.** 1978. A model of evolutionary change in proteins, p. 345–352. *In* M. O. Dayhoff (ed.), Atlas of protein sequence and structure. National Biomedical Research Foundation, Washington, D.C.
14. **del Rey, F., T. F. Donahue, and G. R. Fink.** 1983. The histidine tRNA genes of yeast. J. Biol. Chem. **258**:8175–8182.
15. **Dever, T. E., L. Feng, R. C. Wek, A. M. Cigan, T. F. Donahue, and A. G. Hinnebusch.** 1992. Phosphorylation of initiation factor 2α by protein kinase GCN2 mediates gene-specific translational control of *GCN4* in yeast. Cell **68**:585–596.
16. **Devereux, J., P. Haeberli, and O. Smithies.** 1984. A comprehensive set of sequence analysis programs for the VAX. Nucleic Acids Res. **12**:387–395.
17. **Dieckmann, C. L., and A. Tzagoloff.** 1985. Assembly of the mitochondrial membrane system. J. Biol. Chem. **260**:1513–1520.
18. **Donahue, T. F., A. M. Cigan, E. K. Pabich, and B. C. Valavicius.** 1988. Mutations at a Zn(II) finger motif in the yeast eIF-2β gene alter ribosomal start-site selection during the scanning process. Cell **54**:621–632.

18a. **Dorris, D. R., and E. M. Hannig.** Unpublished data.

19. **Feinberg, A. P., and B. Vogelstein.** 1983. A technique for radiolabeling DNA restriction endonuclease fragments to high specific activity. Anal. Biochem. **132**:6–13. (Addendum, **137**: 266–267, 1984.)
20. **Gribskov, M., and R. R. Burgess.** 1986. Sigma factors from *E. coli*, *B. subtilis*, phage SPO1, and phage T4 are homologous

proteins. Nucleic Acids Res. 14:6745–6763.
21. **Grifo, J. A., S. M. Tahara, M. A. Morgan, A. J. Shatkin, and W. C. Merrick.** 1983. New initiation factor activity required for globin mRNA translation. J. Biol. Chem. **258**:5804–5810.
22. **Gualerzi, C. O., and C. L. Pon.** 1990. Initiation of mRNA translation in prokaryotes. Biochemistry **29**:5881–5889.
23. **Hanahan, D.** 1985. Techniques for transformation of *E. coli*, p. 109–135. *In* D. Glover (ed.), DNA cloning: a practical approach, vol. 1. IRL Press, Oxford.
24. **Hannig, E. M., and A. G. Hinnebusch.** 1988. Molecular analysis of *GCN3*, a translational activator of *GCN4*: evidence for posttranslational control of *GCN3* regulatory function. Mol. Cell. Biol. **8**:4808–4820.
25. **Hannig, E. M., D. J. Thiele, and M. J. Leibowitz.** 1984. *Saccharomyces cerevisiae* killer virus transcripts contain template-coded polyadenylate tracts. Mol. Cell. Biol. **4**:101–109.
26. **Hannig, E. M., N. P. Williams, R. C. Wek, and A. G. Hinnebusch.** 1990. The translational activator GCN3 functions downstream from GCN1 and GCN2 in the regulatory pathway that couples *GCN4* expression to amino acid availability in *Saccharomyces cerevisiae*. Genetics **126**:549–562.
27. **Harashima, S., E. M. Hannig, and A. G. Hinnebusch.** 1987. Interactions between positive and negative regulators of *GCN4* controlling gene expression and entry into the yeast cell cycle. Genetics **117**:409–419.
28. **Harashima, S., and A. G. Hinnebusch.** 1986. Multiple *GCD* genes required for repression of *GCN4*, a transcriptional activator of amino acid biosynthetic genes in *Saccharomyces cerevisiae*. Mol. Cell. Biol. **6**:3990–3998.
29. **Henikoff, S.** 1984. Unidirectional digestion with exonuclease III creates targeted breakpoints for DNA sequencing. Gene **28**:351–359.
30. **Hershey, J. W. B.** 1991. Translational control in mammalian cells. Annu. Rev. Biochem. **60**:717–755.
31. **Hinnebusch, A. G.** 1985. A hierarchy of *trans*-acting factors modulates translation of an activator of amino acid biosynthetic genes in yeast. Mol. Cell. Biol. **5**:2349–2360.
32. **Hinnebusch, A. G.** 1988. Mechanisms of gene regulation in the general control of amino acid biosynthesis in *Saccharomyces cerevisiae*. Microbiol. Rev. **52**:248–273.
33. **Hinnebusch, A. G., and G. R. Fink.** 1983. Repeated DNA sequences upstream from *HIS1* also occur at several other co-regulated genes in *Saccharomyces cerevisiae*. J. Biol. Chem. **258**:5238–5247.
34. **Hoffman, C. S., and F. Winston.** 1987. A ten-minute DNA preparation from yeast efficiently releases autonomous plasmids for transformation of *Escherichia coli*. Gene **57**:267–272.
35. **Ito, H., Y. Fukuda, K. Murata, and A. Kimura.** 1983. Transformation of intact yeast cells treated with alkali cations. J. Bacteriol. **153**:163–168.
36. **Johnston, M., and R. W. Davis.** 1984. Sequences that regulate the divergent *GAL1-GAL10* promoter in *Saccharomyces cerevisiae*. Mol. Cell. Biol. **4**:1440–1448.
37. **Jones, M. D., T. E. Petersen, K. M. Nielsen, S. Magnusson, L. Sottrup-Jensen, K. Gausing, and B. F. C. Clark.** 1980. The complete amino-acid sequence of elongation factor Tu from *Escherichia coli*. Eur. J. Biochem. **108**:507–526.
38. **Kikuchi, Y., H. Shimatake, and A. Kikuchi.** 1988. A yeast gene required for the G_1-to-S transition encodes a protein containing an A-kinase target site and GTPase domain. EMBO J. **7**:1175–1182.
39. **Kinzy, T. G., J. P. Freeman, A. E. Johnson, and W. C. Merrick.** 1992. A model for the aminoacyl-tRNA binding site of eukaryotic elongation factor 1α. J. Biol. Chem. **267**:1623–1632.
40. **Kjeldgaard, M., and J. Nyborg.** 1992. The refined structure of elongation factor Tu from *Escherichia coli*. J. Mol. Biol. **223**:721–742.
41. **Kozak, M.** 1989. The scanning model for translation: an update. J. Cell Biol. **108**:229–241.
42. **Kushnirov, V. V., M. D. Ter-Avanesyan, S. A. Didichenko, V. N. Smirnov, Y. O. Chernoff, I. L. Derkach, O. N. Novikova, S. G. Inge-Vechtomov, M. A. Neistat, and I. I. Tolstorukov.** 1990. Divergence and conservation of *SUP2* (*SUP35*) gene of yeasts *Pichia pinus* and *Saccharomyces cerevisiae*. Yeast **6**:461–472.
43. **Laemmli, U.** 1970. Cleavage of structural proteins during the assembly of the head of bacteriophage T4. Nature (London) **227**:680–685.
44. **Lloyd, M. A., J. C. Osborne, Jr., B. Safer, G. M. Powell, and W. C. Merrick.** 1980. Characteristics of eukaryotic initiation factor 2 and its subunits. J. Biol. Chem. **255**:1189–1193.
45. **London, I. M., D. H. Levin, R. L. Matts, N. S. B. Thomas, R. Petryshyn, and J.-J. Chen.** 1987. Regulation of protein synthesis. Enzymes **18**:359–380.
46. **Lucchini, G., A. G. Hinnebusch, C. Chen, and G. R. Fink.** 1984. Positive regulatory interactions of the *HIS4* gene of *Saccharomyces cerevisiae*. Mol. Cell. Biol. **4**:1326–1333.
47. **Matsudaira, P.** 1987. Sequence from picomole quantities of proteins electroblotted onto polyvinylidene difluoride membranes. J. Biol. Chem. **262**:10035–10038.
48. **Merrick, W. C.** 1992. Mechanism and regulation of eukaryotic protein synthesis. Microbiol. Rev. **56**:291–315.
48a. **Merrick, W. C., and E. M. Hannig.** Unpublished data.
49. **Miller, P. F., and A. G. Hinnebusch.** 1989. Sequences that surround the stop codons of upstream open reading frames in *GCN4* mRNA determine their distinct functions in translational control. Genes Dev. **3**:1217–1225.
50. **Nagashima, K., M. Kasai, S. Nagata, and Y. Kaziro.** 1986. Structure of the two genes coding for polypeptide chain elongation factor 1α (EF-1α) from *Saccharomyces cerevisiae*. Gene **45**:265–273.
51. **Nasmyth, K. A., K. Tatchell, B. D. Hall, C. Astell, and M. Smith.** 1981. Physical analysis of mating-type loci in *Saccharomyces cerevisiae*. Cold Spring Harbor Symp. Quant. Biol. **45**:961–981.
52. **Ovchinnikov, Y. A., Y. B. Alakhov, Y. P. Bundulis, M. A. Bundule, N. V. Dovgas, V. P. Kozlov, L. P. Motuz, and L. M. Vinokurov.** 1982. The primary structure of elongation factor G from *Escherichia coli*. FEBS Lett. **139**:130–135.
53. **Pai, E. F., W. Kabsch, U. Krengel, K. C. Holmes, J. John, and A. Wittinghofer.** 1989. Structure of the guanine-nucleotide-binding domain of the Ha-*ras* oncogene product p21 in the triphosphate conformation. Nature (London) **341**:209–214.
54. **Pathak, V. K., P. J. Nielsen, H. Trachsel, and J. W. B. Hershey.** 1988. Structure of the β subunit of translational initiation factor eIF-2. Cell **54**:633–639.
55. **Perentesis, J. P., L. D. Phan, W. B. Gleason, D. C. LaPorte, D. M. Livingston, and J. W. Bodley.** 1992. *Saccharomyces cerevisiae* elongation factor 2: genetic cloning, characterization of expression, and G-domain modeling. J. Biol. Chem. **267**:1190–1197.
56. **Post, L. E., and M. Nomura.** 1980. DNA sequences from the *str* operon of *Escherichia coli*. J. Biol. Chem. **255**:4660–4666.
57. **Queen, C., and L. J. Korn.** 1984. A comprehensive sequence analysis program for the IBM personal computer. Nucleic Acids Res. **12**:581–599.
58. **Rose, M. D., P. Novick, J. H. Thomas, D. Botstein, and G. R. Fink.** 1987. A *Saccharomyces cerevisiae* genomic plasmid bank based on a centromere-containing shuttle vector. Gene **60**:237–243.
59. **Rothstein, R. J.** 1983. One-step gene disruption in yeast. Methods Enzymol. **101**:202–211.
60. **Sacerdot, C., P. Dessen, J. W. B. Hershey, J. A. Plumbridge, and M. Grunberg-Manago.** 1984. Sequence of the initiation factor IF2 gene: unusual protein features and homologies with elongation factors. Proc. Natl. Acad. Sci. USA **81**:7787–7791.
61. **Sambrook, J., E. F. Fritsch, and T. Maniatis.** 1989. Molecular cloning: a laboratory manual, 2nd ed. Cold Spring Harbor Laboratory, Cold Spring Harbor, N.Y.
62. **Schirmaier, F., and P. Philippsen.** 1984. Identification of two genes coding for the translation elongation factor EF-1α of *S. cerevisiae*. EMBO J. **3**:3311–3315.
63. **Sherman, F., G. R. Fink, and C. W. Lawrence.** 1974. Methods of yeast genetics. Cold Spring Harbor Laboratory, Cold Spring Harbor, N.Y.
64. **Sikorski, R. S., and P. Hieter.** 1989. A system of shuttle vectors and yeast host strains designated for efficient manipulation of DNA in *Saccharomyces cerevisiae*. Genetics **122**:19–27.

65. **Southern, E. M.** 1975. Detection of specific sequences among DNA fragments separated by gel electrophoresis. J. Mol. Biol. **98:**503–517.
66. **Struhl, K., D. T. Stinchcomb, S. Scherer, and R. W. Davis.** 1979. High-frequency transformation of yeast: autonomous replication of hybrid DNA molecules. Proc. Natl. Acad. Sci. USA **76:**1035–1039.
67. **Suzuki, H., E. B. Mukouyama, and T. Kamei.** 1990. Chemical modification of pig liver initiation factor eIF-2 with *N*-ethylmaleimide. Amino acid sequences around the *N*-ethylmaleimide-reactive sulfhydryl groups and the effect of GDP on the modification. J. Biochem. **108:**635–641.
68. **Wek, R. C., M. Ramirez, B. M. Jackson, and A. G. Hinnebusch.** 1990. Identification of positive-acting domains in GCN2 protein kinase required for translational activation of *GCN4* expression. Mol. Cell. Biol. **10:**2820–2831.
69. **Williams, N. P., A. G. Hinnebusch, and T. F. Donahue.** 1989. Mutations in the structural genes for eukaryotic initiation factors 2α and 2β of *Saccharomyces cerevisiae* disrupt translational control of *GCN4* mRNA. Proc. Natl. Acad. Sci. USA **86:**7515–7519.
70. **Wittinghofer, A., and E. F. Pai.** 1991. The structure of Ras protein: a model for a universal molecular switch. Trends Biol. Sci. **16:**382–387.
71. **Yanisch-Perron, C., J. Vieira, and J. Messing.** 1985. Improved M13 phage cloning vectors and host strains: nucleotide sequence of the M13mp18 and pUC19 vectors. Gene **33:**103–119.
72. **Yokota, T., H. Sugisaki, M. Takanami, and Y. Kaziro.** 1980. The nucleotide sequence of the cloned *tufA* gene of *Escherichia coli*. Gene **12:**25–31.